Resource

Cell Host & Microbe

Profiling the Essential Nature of Lipid Metabolism in Asexual Blood and Gametocyte Stages of *Plasmodium falciparum*

Graphical Abstract

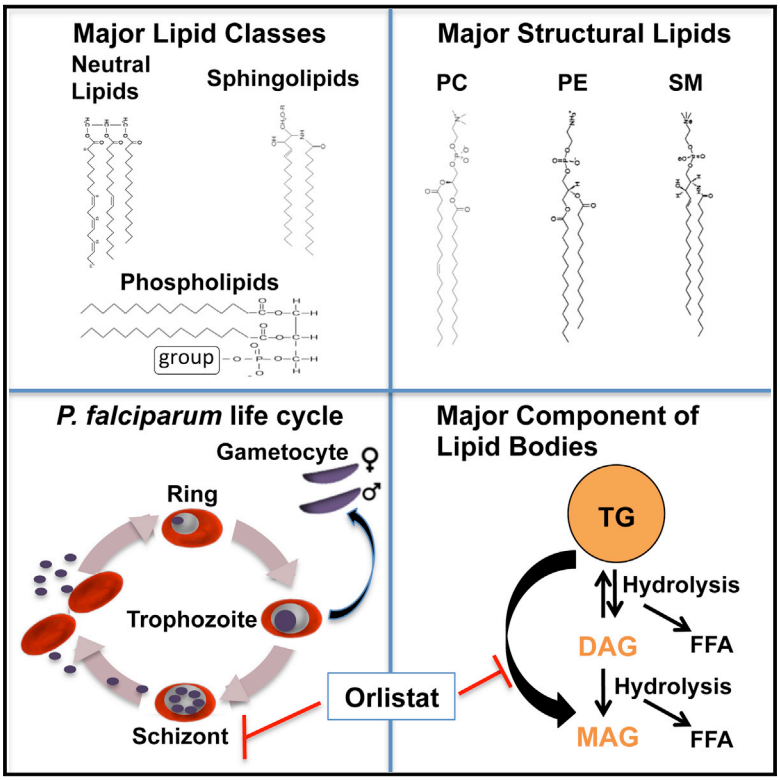

Highlights

- 300 lipids in *Plasmodium falciparum* asexual blood stages and gametocytes were profiled
- Identified lipid classes were synthesized de novo or scavenged from the host
- Triacylglycerols play a key role in asexual parasite maturation
- The identified lipid metabolic pathways are potential targets for future drug discovery

Authors

Sonia Gulati, Eric H. Ekland, Kelly V. Ruggles, ..., Matthias Marti, Gilbert Di Paolo, David A. Fidock

Correspondence

df2260@columbia.edu

In Brief

Plasmodium falciparum malaria parasites undergo rapid proliferation that is fueled by both de novo synthesis and the acquisition of lipids from the host cell. Gulati et al. provide a comprehensive lipid analysis of the pathogenic asexual blood stages and the transmissible gametocyte stages and identify potential targets for drug discovery.

Gulati et al., 2015, Cell Host & Microbe *18*, 371–381
September 9, 2015
http://dx.doi.org/10.1016/j.chom.2015.08.003

Cell Host & Microbe
Resource

Profiling the Essential Nature of Lipid Metabolism in Asexual Blood and Gametocyte Stages of *Plasmodium falciparum*

Sonia Gulati,[1] Eric H. Ekland,[1] Kelly V. Ruggles,[2] Robin B. Chan,[3] Bamini Jayabalasingham,[1] Bowen Zhou,[3] Pierre-Yves Mantel,[4] Marcus C.S. Lee,[1] Natasha Spottiswoode,[1] Olivia Coburn-Flynn,[1] Daisy Hjelmqvist,[4] Tilla S. Worgall,[3] Matthias Marti,[4] Gilbert Di Paolo,[3] and David A. Fidock[1,5,*]
[1]Department of Microbiology and Immunology, Columbia University College of Physicians and Surgeons, New York, NY 10032, USA
[2]Department of Population Health, New York University School of Medicine, New York, NY 10032, USA
[3]Department of Pathology and Cell Biology, Columbia University College of Physicians and Surgeons, New York, NY 10032, USA
[4]Department of Immunology and Infectious Diseases, Harvard School of Public Health, Boston, MA 02115, USA
[5]Division of Infectious Diseases, Department of Medicine, Columbia University College of Physicians and Surgeons, New York, NY 10032, USA
*Correspondence: df2260@columbia.edu
http://dx.doi.org/10.1016/j.chom.2015.08.003

SUMMARY

During its life cycle, *Plasmodium falciparum* undergoes rapid proliferation fueled by de novo synthesis and acquisition of host cell lipids. Consistent with this essential role, *Plasmodium* lipid synthesis enzymes are emerging as potential drug targets. To explore their broader potential for therapeutic interventions, we assayed the global lipid landscape during *P. falciparum* sexual and asexual blood stage (ABS) development. Using liquid chromatography-mass spectrometry, we analyzed 304 lipids constituting 24 classes in ABS parasites, infected red blood cell (RBC)-derived microvesicles, gametocytes, and uninfected RBCs. Ten lipid classes were previously uncharacterized in *P. falciparum*, and 70%–75% of the lipid classes exhibited changes in abundance during ABS and gametocyte development. Utilizing compounds that target lipid metabolism, we affirmed the essentiality of major classes, including triacylglycerols. These studies highlight the interplay between host and parasite lipid metabolism and provide a comprehensive analysis of *P. falciparum* lipids with candidate pathways for drug discovery efforts.

INTRODUCTION

Symptomatic infection by the malaria parasite *Plasmodium* is caused by asexual blood stage (ABS) intra-erythrocytic parasites that undergo cycles of invasion, maturation, replication, and egress. Intra-erythrocytic forms can also enter gametocytogenesis, the sexual differentiation pathway (Nilsson et al., 2015). Gametocytes progress through five morphologically distinctive stages (I–V) over 10–14 days to become transmissible to *Anopheles* mosquito vectors, wherein they undergo fertilization and produce infectious sporozoites. Transcriptomic and proteomic studies have revealed marked differences between gametocytes and ABS parasites (Pelle et al., 2015; Silvestrini et al., 2010).

Throughout its life cycle *P. falciparum* orchestrates a vast array of lipid-dependent processes, including intracellular signaling, protein trafficking, membrane biogenesis, and hemoglobin degradation. Studies have shown that lipid synthesis, uptake, and transport are essential for *P. falciparum* ABS viability (Ben Mamoun et al., 2010). Fatty acids (FAs), the building blocks of lipids, are typically taken up from the human host by ABS parasites, in contrast to mosquito-resident stages that require de novo FA synthesis (van Schaijk et al., 2014). Potent antimalarial activity has been observed with compounds that target membrane or signaling lipids such as phosphatidylcholine (PC), phosphoethanolamine (PE), or phosphatidylinositol (PI) 4-phosphate (Bobenchik et al., 2013; González-Bulnes et al., 2011; McNamara et al., 2013).

To delineate the repertoire and dynamics of *P. falciparum* lipid metabolism, we undertook a comprehensive lipidomics analysis of ABS parasites, microvesicles derived from infected red blood cells (RBCs), gametocytes, and host RBCs. This study identifies potential vulnerabilities that can be leveraged to target malaria infection and transmission and provides a resource for further studies of plasmodial lipids and membrane trafficking.

RESULTS

Comparison of Lipids in *P. falciparum* ABS and Host RBCs

We measured the relative abundance of 304 lipid species in highly synchronized Dd2 parasites, harvested every 8 hr post-invasion (hpi) throughout the 48 hr intra-erythrocytic developmental cycle (IDC). Parasites were isolated following saponin treatment, which lyses RBCs but leaves parasites intact within their plasma membrane. Pelleted parasite samples were washed extensively to remove RBC cytosol and membrane. Lipids were extracted from parasite samples, or control uninfected RBCs, and subjected to liquid chromatography-mass spectrometry (LC-MS). Individual lipid species were assigned to three classes: phospholipids, sphingolipids, and glycerolipids (also referred to as neutral lipids).

Lipidomic comparison of saponin-lysed parasites and uninfected RBCs revealed significant differences in abundance for nearly all of the detected lipid species (Figures 1 and S1 and Table S1). Parasite fractions had levels of phosphatidylglycerol (PG), acyl PG, lysophosphatidylinositol (LPI), bis(monoacylglycero)phosphate (BMP), monosialodihexosyl-ganglioside (GM3), diacylglycerol (DAG), and triacylglycerol (TAG) at least 2-fold higher than those of uninfected RBCs (Figure 1). This suggests that parasites cannot scavenge these lipids without compromising the host and might require de novo synthesis. The other lipids analyzed either displayed a <2-fold difference (e.g., PI) or were enriched in uninfected RBCs (e.g., phosphatidylserine [PS], phosphatidic acid [PA], and ceramide [also known as N-acyl sphingosine]). Lipids enriched in the host cell may serve as a reservoir for parasite-mediated salvage. Indeed, prior studies have shown that *P. falciparum* can import a number of lipid species including ceramide, complex sphingolipids, and Lyso PC (Asahi et al., 2005; Gerold and Schwarz, 2001; Haldar et al., 1991).

Delineating the Temporal Changes of Lipid Species throughout the *P. falciparum* ABS Developmental Cycle

ABS parasites exhibited distinct temporal profiles for all three major lipid classes. Phospholipids, which principally play a structural role, remained relatively constant, with few species changing significantly over time. In contrast, sphingolipid levels decreased and glycerolipid levels increased as ABS parasites matured (Figures 1 and S1A–S1C). The greatest number of lipid species changing $\geq$1.5-fold was between 24 and 32 hpi (Figures S1B and S1C), consistent with rapid growth and increased metabolic activity as the parasite transitioned from ring to trophozoite. Concordant results were observed between our saponin-lysed parasite samples and magnet-enriched trophozoite samples in terms of the abundance of individual lipid species and their levels in parasite versus uninfected RBC samples (Figure S1D).

Phospholipids constituted the major lipid class detected in parasite fractions, with PC and PE together accounting for ~50% of total lipid (Figure 1 and Table S1). A similar finding was also recently reported in a separate study of saponin-lysed parasite samples (Botté et al., 2013). These structural membrane components primarily contained two saturated or monosaturated FA chains (PC [34:1], PC [32:0], and PE [34:1]), consistent with ABS parasites requiring an exogenous supply of oleic (18:1) and palmitic (16:0) acid to sustain growth (Mi-Ichi et al., 2007). We also identified five minor phospholipid subclasses, namely acyl PS, acyl PG, Lyso PI, Lyso PE, and BMP, that were previously uncharacterized in *P. falciparum* (Figures 1 and S1).

Lysophospholipids possess only one FA chain and are minor constituents of cell membranes that in mammalian cells help regulate diverse processes including cell signaling, protein folding, and the mobilization of intracellular Ca^{2+} stores. This subclass made up less than 1% of total parasite lipids and changed rapidly throughout the IDC (Figure 1), consistent with a putative role in intracellular signaling. In cancer lines, Lyso PI promotes cell proliferation and migration (Grzelczyk and Gendaszewska-Darmach, 2013). In *P. falciparum*, Lyso PI exhibited a 2-fold increase at 48 hpi, suggesting a potential role in microtubule-mediated migration of the nucleus into budding merozoites or their subsequent release (Taraschi et al., 1998).

We also observed distinct temporal profiles with the previously uncharacterized phospholipids acyl PS and acyl PG, which peaked early and late, respectively, in the parasite IDC (Figure 1). These lipids had previously been observed in murine brain and bacteria, respectively (Guan et al., 2007; Yagüe et al., 1997). Our in silico analyses (using hidden Markov models) of the *P. falciparum* proteome identified 23% amino acid identity between PF3D7_1212500 and the *Arabidopsis thaliana* acyltransferase At1g78690p, which promotes the accumulation of acyl PG when expressed in *Escherichia coli* (Garrett and Moncada, 2014). Expression of the *PF3D7_1212500* gene peaks at 32 hpi (Bozdech et al., 2003; www.plasmoDB.org), when acyl PG levels begin to increase. The low abundance of acyl PG in humans makes this biosynthetic pathway a potentially attractive target for therapeutic intervention.

Although previously unidentified in *P. falciparum*, BMP has been found in *Leishmania*, where it is proposed to mediate fusion of the parasitophorous vacuole membrane and host autophagosomes (Schaible et al., 1999). In *P. falciparum*, BMP levels suddenly increased at 48 hpi, coincident with merozoite release (Figure 1). We posit that BMP might promote vesicle formation and membrane fusion and remodeling during merozoite egress.

The second major class of lipids observed was sphingolipids, which possess a sphingosine backbone linked to FAs via amide bonds and play critical roles in both membrane structure and signaling (Gault et al., 2010). Sphingomyelin (SM), a structural sphingolipid that aids the biogenesis and maintenance of the tubulovesicular network of membranes (Lauer et al., 1997), was the third most abundant lipid overall, consistent with other studies (Botté et al., 2013; Macrae et al., 2014) (Figure 1). Like other structural lipids, SM levels remained relatively static throughout the IDC (Figure 1). We also detected a previously uncharacterized structural sphingolipid, dihydrosphingomyelin (dhSM; Figures 1 and S1).

SM can also serve as a reservoir for the production of ceramides via its hydrolysis by sphingomyelinases. Ceramides are potent second messengers that regulate diverse processes including cell death, differentiation, and migration (Hannun and Obeid, 2011). Maintaining ceramide homeostasis is paramount for *P. falciparum*, as either insufficient or excessive ceramide levels can have deleterious effects (Labaied et al., 2004; Pankova-Kholmyansky et al., 2003). *P. falciparum* is known to import ceramides (Haldar et al., 1991); however, the evidence for de novo synthesis has been scant. We identified dihydroceramides (dhCer; Figure 1), the biosynthetic precursors of ceramides, suggesting that *P. falciparum* may possess the capability to synthesize ceramide de novo. Ceramides can be modified to produce gangliosides by the addition of an oligosaccharide and a sialic acid. Our study also identified the ganglioside GM3. In humans, gangliosides are concentrated on cell surfaces, where they contribute to cellular recognition, cell-to-cell signaling, and innate immune responses (Ariga et al., 2008). Further studies are warranted to explore the role of GM3 in host-parasite interactions.

ABS parasites possess two major glycerolipid species, DAG and TAG, which consist of a glycerol backbone esterified with FAs. DAG is a potent second messenger that activates protein kinase C (Goñi and Alonso, 1999) and serves as a precursor for major phospholipids and TAG. TAG is packaged into cytosolic

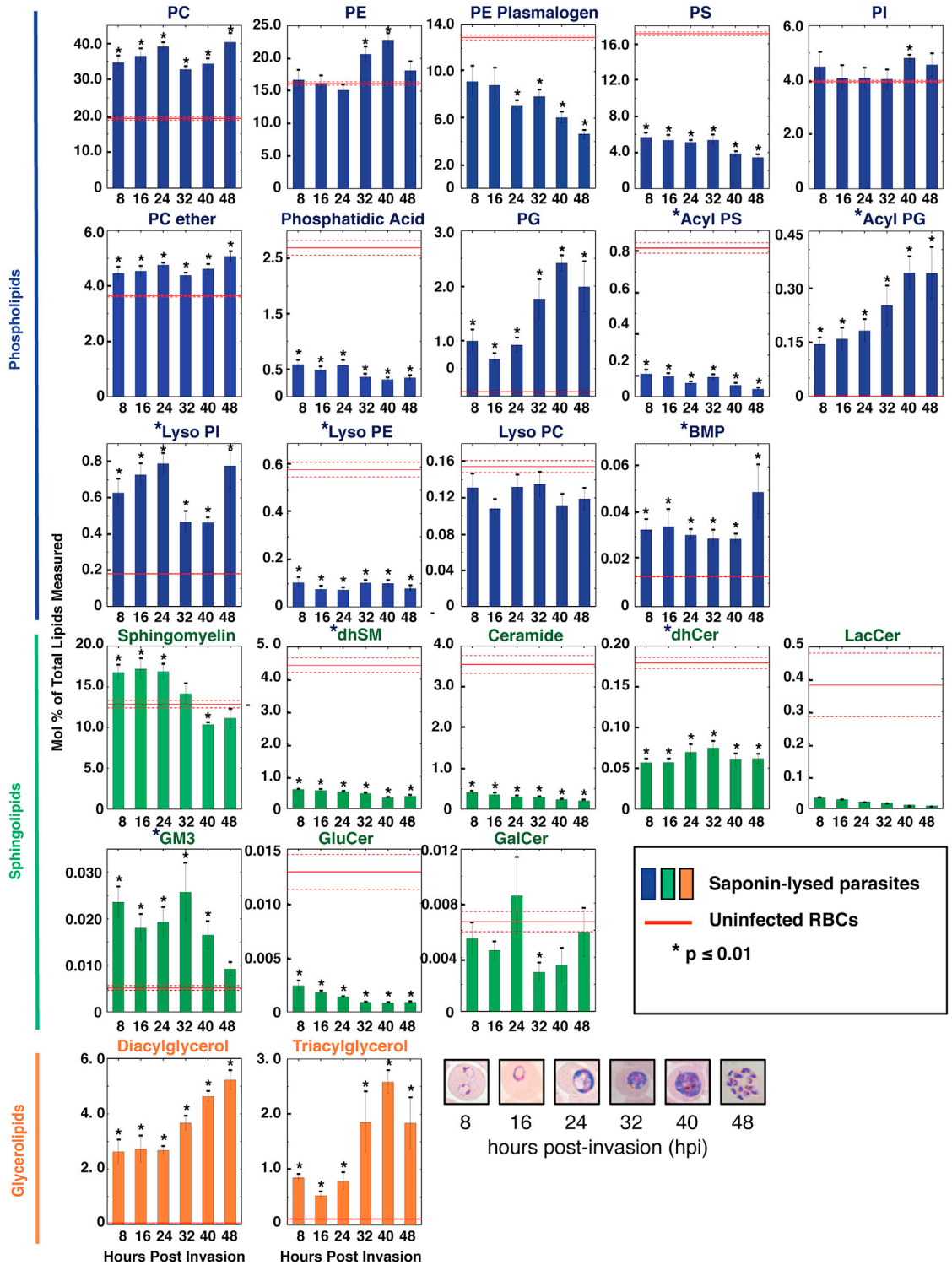

Figure 1. Comparative Profiling of Uninfected Host RBCs and *P. falciparum* ABS Parasites

24 composite lipid species from Dd2 parasites and uninfected human RBCs were quantified via LC-MS/MS. Data are shown as means ± SEM (n = 3 independent experiments performed in triplicate). Uninfected RBCs were harvested at the 48 hr time point. Means and SEM are depicted as solid and dashed red lines, respectively. Significant differences between uninfected RBCs and saponin-lysed ABS parasite pellets (containing some residual RBC membranes) were calculated using Student's t test and are indicated above individual time points; *p ≤ 0.01. Stars beside the names indicate lipid subclasses previously undocumented in *P. falciparum*. PC, phosphatidylcholine; PE, phosphatidylethanolamine; PS, phosphatidylserine; PI, phosphatidylinositol; PG, phosphatidylglycerol; BMP, bis(monoacylglyceryl)phosphate; SM, sphingomyelin; dhSM, dihydroSM; Cer, ceramide; dhCer, dihydroCer; LacCer, lactosylCer; GM3, monosialodihexosylganglioside; GLuCer, GlucosylCer; GalCer, GalactosylCer.

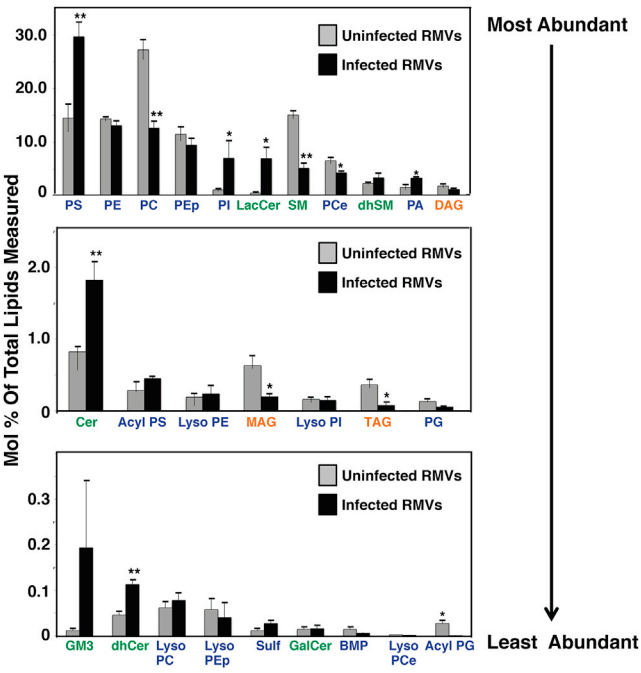

Figure 2. Infected Microvesicles Display a Distinct Lipidomic Profile
27 composite lipid species from uninfected and infected RBC microvesicles (RMVs) were quantified via LC-MS/MS. Data are shown as means ± SEM (n = 3 independent experiments performed in triplicate). Significant difference between uninfected and infected RMVs was calculated by Student's t test. *p ≤ 0.05, **p ≤ 0.01. Abbreviations are listed in the Figure 1 legend, with the following additions: Pep, PE plasmologen; PCe, PC ether; PA, phosphatidic acid; MAG, monoacylglycerol; Sulf, sulfatide.

lipid droplets that detoxify and sequester FAs. In eukaryotic cells, lipase-mediated TAG degradation releases these FAs, which can be used for membrane assembly or beta oxidation (Athenstaedt and Daum, 2006). Both species increased in abundance as the parasite matured (Figure 1B).

Microvesicles Derived from Infected RBCs Display a Distinct Lipid Profile

We also characterized the lipid profiles of RBC-derived microvesicles (RMVs, also referred to as exosome-like vesicles or microparticles) purified from infected and uninfected RBCs (Figures 2 and S2). Microvesicles mediate intercellular communication and the transfer of lipids, cytosolic proteins, and RNA in mammalian cells (Raposo and Stoorvogel, 2013). Patients infected with *P. falciparum* possess elevated levels of RMVs, which have been implicated in intercellular communication and gametocytogenesis (Mantel et al., 2013; Nantakomol et al., 2011; Regev-Rudzki et al., 2013). RMVs derived from infected RBCs (iRMVs) were significantly enriched for PS and PI. PS was 2-fold higher in infected, relative to uninfected, RMVs; this increase appeared to come primarily at the expense of PC (Figure 2). These data corroborate previous evidence of elevated PS levels in RMVs from *P. falciparum* cultures or plasma of *P. falciparum*-infected humans or *P. berghei*-infected mice (Couper et al., 2010; Mantel et al., 2013; Nantakomol et al., 2011). RMVs have been proposed to arise by blebbing from specific subdomains, potentially lipid rafts, within the RBC membrane. *P. falciparum*-infected RBC membranes and lipid rafts are both enriched in PS, which could provide the source of phospholipid detected in these iRMVs (Mantel et al., 2013; Pattanapanyasat et al., 2010; Salzer and Prohaska, 2001). iRMVs were also enriched for sphingolipids including ceramide, lactosylceramide (LacCer), dhCer, and GM3. Ceramide, LacCer, and GM3 are potent signaling molecules that modify the immune response (Inokuchi et al., 2015; Maceyka and Spiegel, 2014); these may contribute to the immunomodulatory effects ascribed to *P. falciparum* iRMVs (Mantel et al., 2013).

The Antimalarial Agent Orlistat Inhibits the Hydrolysis of Triacylglycerols

To further probe the contribution of lipid metabolism to *Plasmodium* ABS viability, we assessed the antiparasitic activity of 21 compounds known to inhibit various lipid metabolic pathways in other organisms (Table S2). 72 hr growth inhibition studies revealed moderate to potent antimalarial activity for Orlistat and GW4869 (yielding mean ± SEM IC_{50} values of 0.9 ± 0.1 μM and 6.0 ± 0.3 nM, respectively).

Orlistat is an irreversible inhibitor of pancreatic lipase, which hydrolyzes TAGs to a monoglyceride molecule and two FA species. This anti-obesity drug is known to inhibit *P. falciparum* ABS growth (Yuan et al., 2011; Figure 3A and Table S2). To examine its stage specificity, we added Orlistat at 8× IC_{50} to highly synchronized ring-stage Dd2 parasites and monitored development every 8 hr. Orlistat had no effect on ring to trophozoite progression, yet dramatically stalled parasite growth at the schizont stage 48–56 hpi (Figure 3B). The effect was specific, as adding Orlistat at 48 hpi (after the onset of merozoite formation) did not prevent merozoite release or RBC reinvasion. This arrest coincides with a significant drop in TAG levels at 48 hpi (Figure 1) and with peak transcription of *PF3D7_1427100* that encodes a putative lipase (Bozdech et al., 2003). The addition of exogenous oleic acid (18:1) and palmitic acid (16:0) did not rescue Orlistat-treated parasites (Figure S3A), suggesting that the rapid and localized intracellular release of FAs is essential for parasite development late in the ABS cycle.

To directly assess whether Orlistat impacted TAG levels late during ABS development, we co-incubated synchronized parasites, beginning at 6–8 hpi, with 8× IC_{50} concentrations of Orlistat as well as the FA tracer [^{3}H]-oleic acid (18:1). Parasites were then harvested at 24 hpi and 56 hpi time points; at 56 hpi, schizonts had stalled and parasite reinvasion had not occurred (Figures 3B and 3C). As controls, we used an unrelated drug azithromycin, which targets the apicoplast 50S ribosomal subunit and causes a delayed death phenotype (treated parasites die in the subsequent cycle of RBC infection; Sidhu et al., 2007). Parasites were harvested after 72 hr of exposure, corresponding to 30–32 hpi in the second cycle of growth and a time at which their development had stalled, as well as an initial time point of 24 hpi. Using thin-layer chromatography, TAG levels in drug-treated samples were calculated relative to DMSO-treated controls. For both Orlistat and azithromycin at 24 hpi, TAG levels in drug-treated parasites were comparable to those of DMSO-treated controls (Figure 3C). Once parasites had stalled, however, Orlistat-treated parasites had significantly higher TAG levels than azithromycin-treated parasites

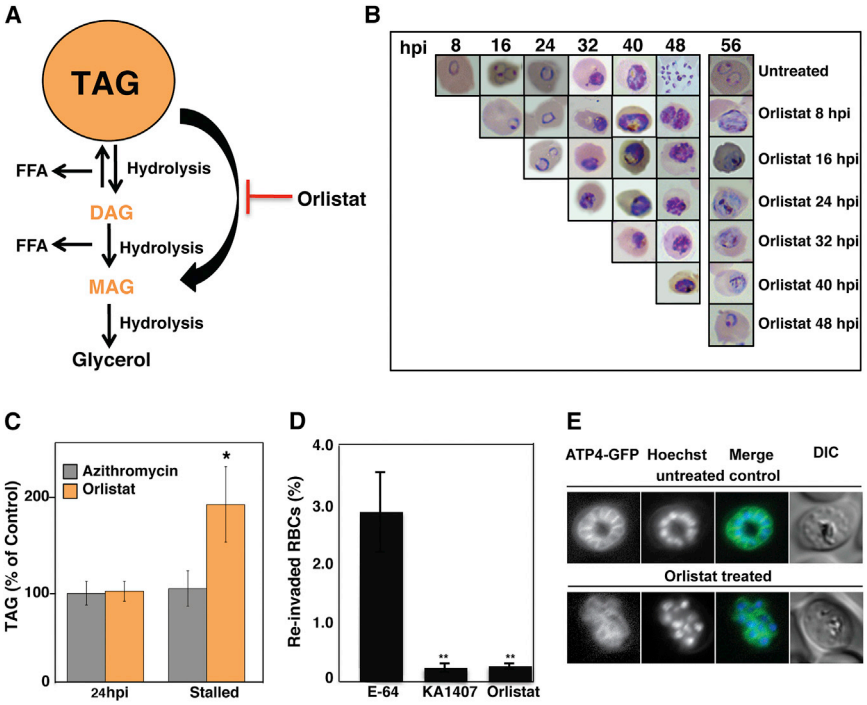

Figure 3. Orlistat Inhibits Triacylglycerol Degradation and Merozoite Maturation

(A) Schematic representation of TAG degradation. TAG is stored in cytosolic lipid droplets (orange) and can be degraded by lipases to produce DAG or MAG. Orlistat prevents TAG catabolism by inhibiting lipase action.

(B) Highly synchronized ABS parasites (starting at 8 hpi) were serially assessed for development every 8 hr following the addition of 6 μM Orlistat (8× IC_{50}), beginning at 8, 16, 24, 32, 40, and 48 hpi. Once added, Orlistat was maintained until the final time point at 56 hpi. Giemsa-stained smears were analyzed by light microscopy (examples provided), and the experiment was performed on three separate occasions. Across all experiments, parasites averaged 2.5%–4% until reinvasion at 48 hr, when untreated parasites reinvaded and parasitemia climbed to 9%–12%. However, reinvasion did not occur in Orlistat-treated parasites, and parasitemias remained at 2%–2.5%.

(C) Synchronized ABS parasites were treated 6–8 hpi with [^{3}H]-oleic acid (18:1) and 8× IC_{50} concentrations of either Orlistat or the delayed death inhibitor azithromycin. DMSO was used as a solvent control. Parasites were harvested after 24 hr. For Orlistat and azithromycin, parasites were also harvested after a further 24 or 48 hr (corresponding to 54–56 hpi or 78–80 hpi), respectively. For these agents, parasites had developmentally stalled at the later time points (late in the first and second cycles of growth, respectively). Lipids were extracted and subjected to thin-layer chromatography. TAG levels were normalized to DMSO-treated parasites extracted at the corresponding time points and are shown as means ± SEM (n = 3 independent experiments performed in triplicate).

(D) Percent reinvasion of RBCs after mechanical rupture of synchronized schizont-infected RBCs treated with 1 μM E-64, 125 nM KAI407, or 6 μM (8× IC_{50}) Orlistat. Data are shown as means ± SEM (from three independent experiments performed in triplicate).

(E) Plasma membrane ingression around developing daughter cells was visualized using the plasma membrane marker PfATP4-GFP (McNamara et al., 2013). Synchronized parasites were treated at 24 hpi with either 6 μM Orlistat or DMSO and imaged 28 hr later (i.e., 52 hpi). Control parasites had organized and fully enclosed developing merozoites, whereas plasma membrane ingression was perturbed by Orlistat treatment. Nuclei were stained with Hoechst 33342.

(Figure 3C). These data were confirmed in separate experiments that measured TAG levels by mass spectrometry (Figure S3B). Our findings are consistent with the hypothesis that parasites need to hydrolyze TAG to progress late in the ABS cycle.

TAG hydrolysis produces a rapid increase in intracellular FAs in ABS parasites (Palacpac et al., 2004a). These FAs may promote the formation of membranes during merozoite maturation, or due to their detergent-like properties may mediate the rupture of RBC membranes releasing fully mature merozoites. To distinguish between these hypotheses, we assessed whether Orlistat-treated merozoites are viable once released by mechanical disruption. We added Orlistat (8× IC_{50}) to a highly synchronized Dd2 culture at 38–40 hpi, prior to maximal TAG degradation (Figure 1). At 50–56 hpi, the stalled parasites were mechanically ruptured to release merozoites. As a positive control, we utilized 1 μM E-64, a cysteine protease inhibitor that blocks parasite egress but does not prevent reinfection by mechanically released merozoites (Boyle et al., 2010; Drew et al., 2008). As a negative control we used 125 nM of KAI407 (5× IC_{50}), a phosphatidylinositol-4-kinase inhibitor that impairs cytokinesis and causes defective merozoite membrane biogenesis (McNamara et al., 2013). E-64 and KA1407 were added once merozoites began to form. As anticipated, E-64-treated parasites reinvaded RBCs following rupture, resulting in a parasitemia of ~3%. In contrast, rupture of Orlistat-treated parasites yielded a 10-fold lower parasitemia, similar to KAI407-treated parasites (Figure 3D). These data suggest that Orlistat acts prior to merozoite egress.

To examine whether Orlistat-treated parasites were unable to form merozoite membranes and therefore mature, we visualized the invagination of the parasite plasma membrane around developing merozoites using the plasma-membrane protein PfATP4-GFP (Rottmann et al., 2010). Parasites were treated with 6 μM Orlistat at the 24 hr time point (as in Figure 3B) and imaged after 28 hr of incubation when they had progressed to late schizonts. DMSO-treated controls displayed complete ingression of the plasma membrane. In comparison, Orlistat-treated parasites had disorganized segmentation and lacked fully defined merozoites (representative results shown in Figure 3E). These data suggest that Orlistat inhibits merozoite maturation prior to egress and that TAG hydrolysis plays an important role in this maturation process.

GW4869 Possesses Potent Antimalarial Activity

Neutral sphingomyelinase (SMase) hydrolyzes sphingomyelin to produce ceramide in response to cellular stress (Figure 4A). Neutral SMase activity has been detected in *P. falciparum* and is inhibited by low micromolar concentrations of scyphostatin, a first-generation neutral SMase inhibitor (Hanada et al., 2000). We tested five newer, structurally different neutral SMase inhibitors for inhibition of ABS parasite growth. Among these, GW4869 had potent antimalarial activity with an IC_{50} value of

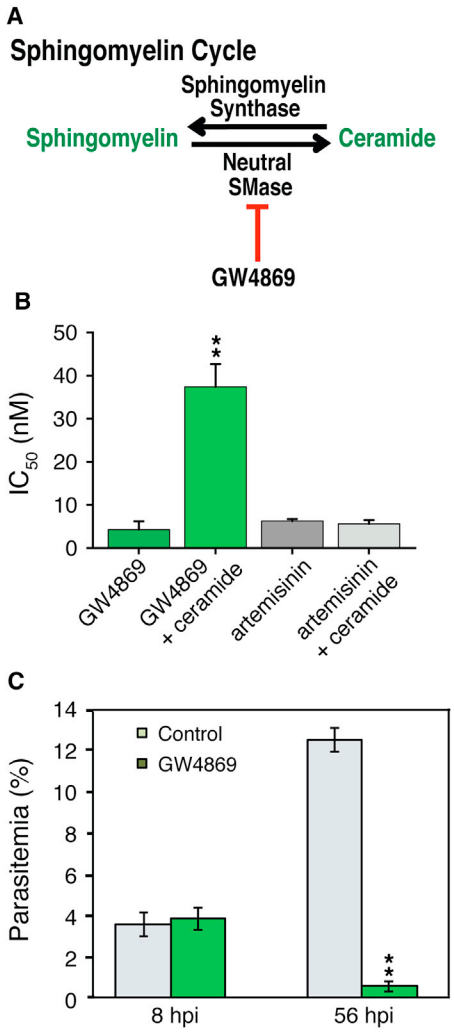

Figure 4. GW4869 Interferes with ABS Ceramide Metabolism and Infected RMV Egress

(A) Schematic representation of the sphingomyelin cycle. Ceramide is produced via the hydrolysis of sphingomyelin via a neutral sphingomyelinase, which is inhibited by GW4869.

(B) Dd2 parasites were subjected to 72 hr drug assays with GW4869 ± 50 μg/ml of lignoceric ceramide. Mean ± SEM IC_{50} values were calculated from four independent sets of duplicates. **p ≤ 0.01.

(C) Parasite ABS development was assessed following the addition of 1 μM GW4869 (~170× IC_{50}) to highly synchronized parasites, beginning 8 hpi. Compound was added at time points 8, 16, 24, 32, 40, or 48 hpi. Giemsa-stained smears were counted at every time point, as well as the final 56 hpi time point (experiment performed in duplicate on two separate occasions). Mean ± SEM parasitemias are shown for the 8 and 56 hpi time points. **p ≤ 0.01.

6 nM (Figure 4B and Table S2). This effect was partially rescued by supplementation of GW4869-treated parasites with exogenous lignoceric acid (C24:0) ceramide, the most abundant ceramide species in *P. falciparum* ABS parasites (Figure 4B and Table S1). In control experiments, lignoceric ceramide had no effect on artemisinin activity (Figure 4B). These data suggest that GW4869 exerts its antiparasitic activity by inhibiting ceramide production.

To determine when parasites are most sensitive to GW8469 treatment, we exposed highly synchronized Dd2 cultures to 1 μM of GW4869 shortly following merozoite invasion and monitored parasite expansion and development every 8 hpi. Parasites continued to develop throughout the ABS cycle in the presence of drug. Significantly fewer drug-treated parasites were observed after reinvasion (at 56 hpi; Figure 4C). Untreated control parasites successfully reinvaded and increased the parasitemia to ~12%, a 4-fold increase (at 8 hpi). In our growth inhibition assays, GW4869 never achieved 100% killing even at the highest dose of 500 μM. We posit that a small population of parasites can survive by scavenging ceramide from RBCs, therefore potentially limiting the utility of SMase inhibitors as therapeutics.

Lipids Play a Role in Gametocyte Development and Induction

The switch from the proliferating ABS to the non-proliferating gametocyte is essential for *Plasmodium* transmission to the mosquito vector. To characterize gametocyte lipid metabolism and how it varies from its asexual precursor, we measured the relative abundance of lipid species in early- and late-stage gametocytes, shown as $\log_2$ fold change from a trophozoite (32 hpi)-enriched ABS culture (Figures 5A and S4 and Table S3). We found that the gametocyte lipidome, like its transcriptome and proteome, varies significantly from its ABS precursor. Approximately 70% of the lipid classes measured exhibited a significant difference in abundance from 32 hpi trophozoites (Figure 5A). Moreover, a similar number of lipids also displayed marked changes in abundance between early- and late-stage gametocytes, suggesting that lipid metabolic pathways are active throughout gametocyte maturation.

We observed a general reduction in phospholipid abundance in gametocytes, with 67% of these lipids significantly reduced in both early and late stages as compared to ABS trophozoites (Figure 5A). Lysophospholipids experienced the greatest decrease in relative abundance, with ether lysophosphatidylcholine (LPCe) exhibiting a 6-fold and 4-fold decrease during early and late gametocytogenesis, respectively (Figure 5A). These findings are concordant with transcriptional evidence of upregulation of a putative lysophospholipase PFI1775W by AP2-G, a master regulator of gametocyte development (Kafsack et al., 2014). In contrast, PS exhibited an 8-fold increase in early-stage gametocytes as compared to ABS parasites. This is consistent with the high level of expression of the putative PS synthase PF3D7_1366800 throughout gametocytogenesis (www.plasmoDB.org). Based on these data, we propose that both PFI1775W and PF3D7_1366800 might serve as potential gametocytocidal targets.

Almost all of the sphingolipids measured exhibited a significant increase in relative abundance in gametocytes, with the exception of GM3. Specifically, we saw a dramatic expansion in ceramides and complex sphingolipids (Figure 5A). The most significant change occurred with the ceramide precursor, dhCer, which increased 4- to 10-fold in early- and late-stage gametocytes, respectively. Increased dhCers in gametocytes suggest an increased requirement for sphingolipids that cannot be met by uptake alone.

Conversely, glycerolipids were less abundant in gametocytes than in ABS parasites (Figure 5A). TAG in particular was decreased

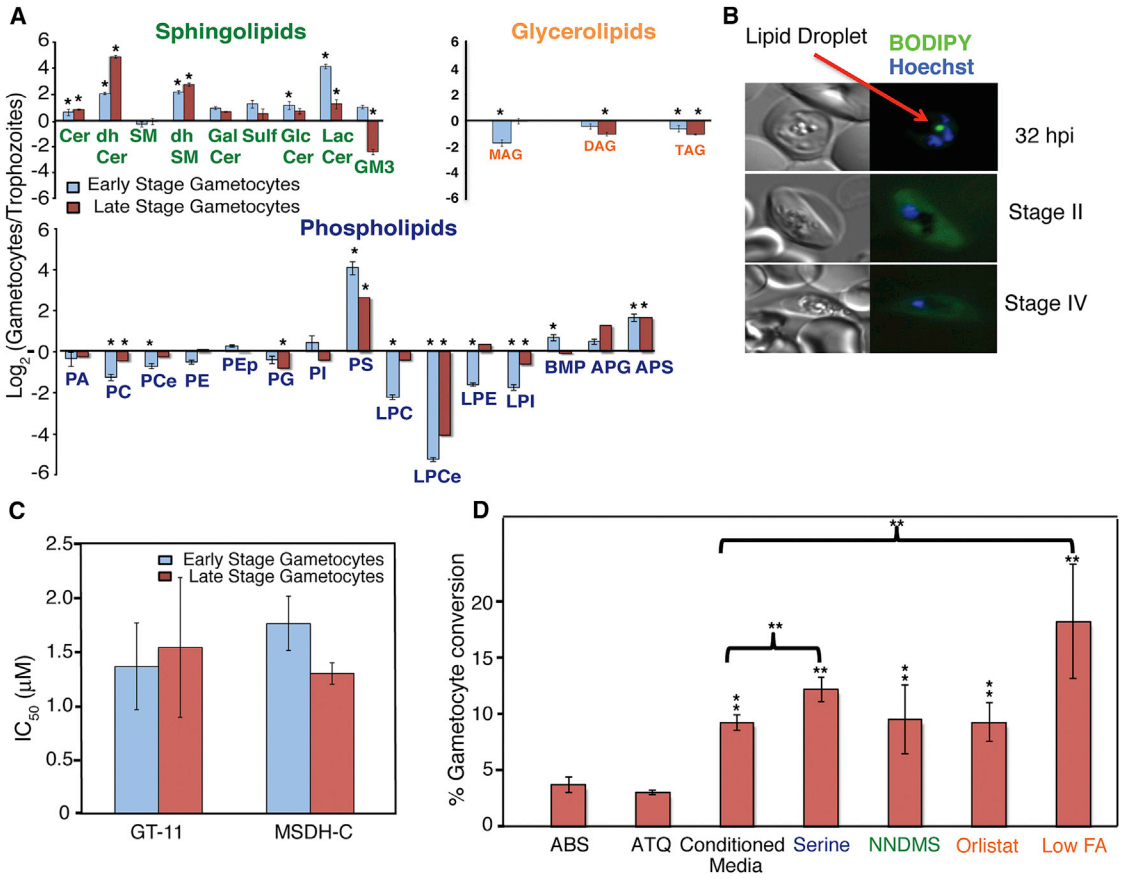

Figure 5. Gametocytes Possess a Unique Lipidomic Profile That Contributes to Their Induction and Development

(A) LC-MS/MS was used to quantify 27 lipid classes from saponin-lysed early-stage (stages I–II) and late-stage (stages IV–V) gametocytes, and trophozoites (32 hpi). The relative abundance of the 27 lipid classes is presented as $\log_2$ gametocytes/trophozoites. Data show means ± SEM (n = 3 independent experiments performed in triplicate). Significant differences between trophozoite and gametocytes were calculated using the Student's t test. *p ≤ 0.05, **p ≤ 0.01.

(B) Cytosolic lipid droplets were stained with BODIPY 493/503 in Dd2 ABS parasites (32 hpi) or gametocytes (early and late stages). Nuclei were stained with Hoechst 33342. The red arrow indicates the presence of a cytosolic lipid droplet in the 32 hpi trophozoite. Representative images from a single experimental replicate are shown (n = 2 independent experiments).

(C) Early- or late-stage gametocytes were treated with the indicated compounds for 3 days. IC_{50} values were calculated based on the quantification of viable gametocytes by flow cytometry. Data show mean ± SEM IC_{50} values (n = 3 independent experiments performed in duplicate).

(D) Gametocytes were induced by stressing ABS parasites with atovaquone (1.25 nM for 24 hr), 50% conditioned media (for 24 hr), serine (500 μM for 48 hr), NNDMS (2 μM for 24 hr), Orlistat (0.8 μM for 24 hr), or media with low FAs (15 μM of each of palmitic and oleic acid). ABS parasites (day 0) and gametocytes (days 10–12) were quantified by flow cytometry. Data are presented as a percent of ABS parasites on day 0 that became gametocytes. Data show means ± SEM (n = 3 independent experiments performed in triplicate). **p ≤ 0.01.

in both early- and late-stage gametocytes. To assess the status of lipid droplets, which are TAG-storing organelles, we stained early- and late-stage gametocytes with BODIPY 493/503, a glycerolipid-specific dye. We observed distinct foci of BODIPY staining in trophozoites, indicating the presence of cytosolic lipid droplets (typically one per parasite). In contrast, BODIPY staining in early and late gametocytes was diffuse and weak, suggesting the absence of droplets (Figure 5B). These data suggest that unlike ABS parasites, gametocytes do not amass TAG stores. In mammalian cells, lipid droplets can serve as a FA reservoir to furnish heightened metabolic needs (Barbosa et al., 2015). In gametocytes, however, many of the major structural lipids (i.e., PC, PE, or SM) were significantly lower or remained constant, suggesting that membrane proliferation or remodeling occur less than in ABS parasites, thereby decreasing FA requirements.

To better understand which lipid metabolic pathways are critical for gametocyte viability, we tested our panel of 21 lipid-targeting compounds (Table S2) for gametocytocidal activity. The potent gametocytocidal agent methylene blue was included as a positive control (Adjalley et al., 2011). Only two of the compounds assayed, GT11 and MSDH-C, exhibited gametocytocidal activity (Figure 5C). Both of these compounds target dhCer synthase in the de novo ceramide synthesis pathway (Table S2). These data support our lipidomic findings that ceramide synthesis increases in gametocytes and may play an essential role in gametocyte viability.

The physiological mechanism that prompts sexual conversion of asexual parasites in vivo is undoubtedly multifactorial. Recent studies have illustrated that one such factor is iRMVs, present in conditioned medium (Mantel et al., 2013; Regev-Rudzki et al.,

2013). In our studies iRMVs and gametocytes showed similar lipidomic profiles. Notably, both were enriched in dhCer, ceramide, and PS (Figures 2 and 5A). To explore ceramide and PS metabolism in gametocytogenesis, we treated highly synchronized cultures enriched for rings (with a 3% parasitemia, starting on day −2) with 500 μM exogenous serine or 2 μM N,N-Dimethylsphingosine (NNDMS). Serine was chosen, as it increases intracellular levels of certain phospholipids (including PS and PE) and sphingolipids (Elabbadi et al., 1997; Slotte, 2013). We selected NNDMS, as it targets ceramide metabolism in ABS parasites by decreasing ceramide catabolism to sphingosine-1-phosphate (S1P; see below). This most likely occurs via the documented ability of NNDMS to inhibit sphingosine kinases that convert sphingosine to S1P (Igarashi et al., 1990). As an unrelated control drug, we used atovaquone, an inhibitor of cytochrome B in the parasite mitochondrion. As a positive control, we supplemented an 8%–10% ring-stage parasite culture with 50% conditioned media, which is a standard means of inducing gametocytes (Fivelman et al., 2007). Upon reinvasion (day 0), all cultures were also treated with 50 mM N-acetyl glucosamine (NAG) for 4–6 days to eliminate ABS parasites. We observed significantly more gametocytes in low-density cultures supplemented with exogenous serine than in high-parasitemia cultures treated with 50% conditioned media (Figure 5D). Furthermore, the addition of NNDMS to low-density cultures induced a number of gametocytes comparable to that induced with conditioned media treatment (Figure 5D). Our mass spectrometry studies also revealed that early- to mid-stage gametocytes contain low levels of S1P as compared to asexual ring-stage parasites. These studies identified mean ± SEM levels of 2,128 ± 468 picomoles of S1P/mg of total parasite protein for untreated gametocytes, as compared with 4,471 ± 737 for NNDMS-treated ABS parasites and 9,911 ± 3,295 for untreated ABS parasites (S1P levels compared with untreated ABS parasites were significantly different for both other groups; see Supplemental Information). Those studies corroborate the importance of diverting ceramide away from its catabolism to S1P (via sphingosine). Collectively, these data suggest that manipulating sphingolipids and phospholipid metabolic pathways may shift the balance toward gametocytogenesis.

We next asked whether modifying glycerolipid metabolism in ABS parasites might increase gametocytogenesis. This was prompted by our observations of increased gametocytemia in cultures treated with the TAG lipase inhibitor Orlistat. Similar to the experiments described above, we treated a highly synchronized culture enriched for rings (3% parasitemia) with 800 nM Orlistat for 24 hr. This treatment produced equivalent numbers of gametocytes compared to cultures treated with 50% conditioned media (Figure 5D). This result suggests that inhibiting the mobilization of FA stores from lipid droplets in ABS parasites favors sexual-stage development. This corroborates a prior study demonstrating that disruption of an ATP-binding cassette transporter, ABCG2, in ABS parasites decreased glycerolipids and promoted gametocytogenesis (Tran et al., 2014). In eukaryotes, lipid droplets protect against cell death during times of nutrient deprivation by providing FAs to meet the metabolic and energy needs of the cell (Cabodevilla et al., 2013). We conjecture that the inability of Orlistat-treated ABS parasites to access their reserve stores of FAs mimics a FA deficit, and therefore a nutrient-poor environment, stimulating gametocytogenesis. Consistent with this possibility, we observed that exposing ABS parasites to diminished exogenous FA levels by culturing with 15 μM palmitic acid (C16:0) and oleic acid (C18:1) in the absence of human serum or Albumax produced significantly more gametocytes than our 50% conditioned media positive control (Figure 5D).

DISCUSSION

Our lipidomic analysis has identified lipid classes that were previously uncharacterized in *P. falciparum*. These lipids include 6 phospholipid (lyso PE, lyso PI, ether lyso PC, acyl PG, acyl PS, and BMP) and 4 sphingolipid (dhSM, dhCer, GM3, and sulfatides) classes. Overall, 75% of the detected lipid classes exhibited significant changes in abundance throughout the ABS life cycle, with 9 lipids exhibiting a change greater than 2-fold. Furthermore, a majority of the lipids measured are abundant in the RBC, providing a potential pool of lipids that can be scavenged by the parasite.

One important extrapolation from our data is that lipid metabolism *in P. falciparum* is not insular, but is instead dynamically intertwined with that of its host. This was exemplified by our studies with GW4869, which inhibits the parasite's ability to produce ceramide via the hydrolysis of sphingomyelin. GW4869 failed to kill 100% of parasites even at 170× IC_{50}, and supplementation with exogenous ceramide further countered the effects of the compound. We estimate that ceramide makes up 3.5% of total host RBC lipids, i.e., ∼10 times more than that found in the parasite. While GW4869 clearly had potent antimalarial activity, we posit that a small population of parasites survived by acquiring ceramide from the host. Therefore, the neutral SMase pathway alone is likely not a primary candidate for future antimalarial drug discovery work.

In contrast, our analysis identified four lipid classes, TAG, DAG, PG, and acyl PG, as potential limiting factors for parasite survival. Each demonstrated a significant increase in abundance throughout the ABS cycle, suggesting their importance in parasite growth and development. Equally notable, these lipids are not abundant in the RBC, preventing the parasite from scavenging these lipids without cannibalizing its host. Previous unsuccessful attempts to genetically disrupt the TAG biosynthetic pathway (Palacpac et al., 2004b) corroborate our studies with Orlistat, indicating the importance of TAG metabolism to parasite development. Our findings with GW4869 and Orlistat highlight the necessity to understand the interplay between host and parasite lipid metabolic networks when assessing the therapeutic potential of a lipid-targeting drug. In this case, although Orlistat (IC_{50} 0.9 μM) is less potent than GW4869 (IC_{50} 6 nM), it is arguably a better drug candidate as it targets the metabolic pathway of a lipid that cannot be scavenged.

To identify lipid metabolic pathways that may serve as gametocytocidal targets, we profiled the lipidome of early-stage (stages I–II) and late-stage (stages IV–V) gametocytes. Overall, 70% of the lipid classes under investigation varied significantly in abundance between early and late stages, suggesting that lipid metabolic pathways are active throughout sexual-stage maturation. A similar number of differences were observed between gametocytes and ABS parasites. Specifically, we found

that relative to the trophozoite, both early- and late-stage gametocytes were enriched for sphingolipids involved in ceramide metabolism while possessing fewer phospholipids and glycerolipids. These data were corroborated by our finding that MSDH-C and GT11, inhibitors of the ceramide biosynthetic pathway, killed gametocytes with an IC_{50} in the 1–2 μM range. Neither compound was active against ABS parasites, highlighting the singular importance of de novo synthesis of ceramides to gametocyte viability. The antimalarial GW869, which inhibits a neutral SMase, had no effect on gametocytes. This suggests that perhaps the primary pathway for ceramide production in gametocytes has shifted away from sphingomyelin hydrolysis to de novo synthesis of ceramide.

Multiple factors likely contribute to the onset of gametocytogenesis. Our lipidomics analysis revealed that gametocytes are highly enriched for PS and ceramides, while having lower levels of glycerolipids. Consequently, we hypothesized that these pathways may play a role in creating a lipid environment that favors gametocyte induction. Our studies show that the addition of serine or NNDMS, which increases various phospholipids and sphingolipids, can increase gametocyte induction. Exogenous serine may promote gametocytogenesis via the perturbation of phospholipid or sphingolipid pathways. Treatment of parasites with NNDMS also resulted in increased gametocyte numbers and decreased S1P levels, evoking a potential role for ceramide metabolism in gametocytogenesis. We have also shown that altering glycerolipid metabolism, by treating with Orlistat or depleting levels of exogenous FAs, increases gametocytemia. These data indicate that lipid depletion, including FA constituents, might be an important cue for gametocytogenesis commitment.

With malaria still a leading cause of infectious disease morbidity and mortality, it is essential that we define core features of *Plasmodium* biology. The ability to generate concurrent lipidomic, transcriptomic, and proteomic profiles will allow us to dissect metabolic networks that underlie the molecular etiology of malaria, as an approach to expanding our therapeutic armamentarium.

EXPERIMENTAL PROCEDURES

P. falciparum Asexual Blood-Stage Cultures and Synchronization and Saponin Lysis

Parasites were maintained in human RBCs in RPMI 1640 complete medium containing 10% human serum or 0.5% Albumax (for NF54 and Dd2 strains, respectively). Strains were synchronized with 5% D-sorbitol (w/v) for two or more successive growth cycles and expanded to 8%–10% parasitemia prior to harvesting. For lipid analysis, 75 ml cultures were prepared at 8%–10% parasitemia and 4%–6% hematocrit. Cultures were centrifuged and the medium removed. Cell pellets were resuspended in 40 ml of 1× PBS buffer with 0.1% saponin and incubated for 10–15 min. Cells were then recentrifuged to pellet the parasites, colored brown because of the internal hemozoin. A white layer of RBC membrane that sediments above the parasite pellets was carefully removed along with the supernatant. Parasite pellets (typically 0.5–1.0 ml) were washed an additional 3–4 times with 15 ml 1× PBS buffer. These washes removed residual hemoglobin and RBC membrane, ensuring a minimal RBC component in the final saponin-lysed parasite fraction.

Gametocyte Commitment and Harvesting

To produce gametocytes, 300 ml cultures of ABS NF54 parasites were doubly synchronized with 5% D-sorbitol (w/v) treatment. 2%–3% synchronous trophozoites were incubated overnight to obtain 8%–10% ring-stage parasites. Cultures were stressed by replacing 50% of the spent medium with fresh medium (resulting in "50% conditioned media"). On the next day (day −1), when parasites reached the trophozoite stage, the medium was changed and cultures were diluted 2-fold. On the following day, day 0, 50 mM N-acetyl glucosamine (NAG) was added to ring-stage parasites and maintained for 2–3 cycles to eliminate ABS forms. Immature gametocytes (stages I–II) and mature gametocytes (stages IV–V) were harvested on days 2–4 and 10–12, respectively. Harvested cultures were lysed with 0.01% saponin, washed 3–4 times with 1× PBS, and frozen. Gametocytemias at time of harvest were 3%–4%.

Analysis of Lipids Using High-Performance Liquid Chromatography-Mass Spectrometry

Lipids were extracted from uninfected RBCs, RBC microvesicles, Dd2 parasites, and gametocytes, as described (Hara and Radin, 1978). Briefly, 2 ml of isopropanol: hexane (1:2) and 2 ml of KCl (2 M): MeOH (4:1) were added to cell pellets. Samples were mixed and centrifuged at 4,000 RPM for 5 min. The organic (top) layer was removed and the pellet was re-extracted with 2 ml of isopropanol: hexane (1:2). The organic phase was dried with nitrogen gas and resuspended in 500 μl hexane (Tinkelenberg et al., 2000). Samples were dried down again with nitrogen gas and resuspended in 300 μl chloroform: methanol (2:1). Lipid extracts were analyzed using a 6490 Triple Quadrupole LC/MS system and were spiked with appropriate internal standards. Glycerophospholipids and sphingolipids were separated with normal-phase HPLC. An Agilent Zorbax Rx-Sil was used under the following conditions: mobile phase A (chloroform: methanol: 1 M ammonium hydroxide, 89.9:10:0.1, v/v) and mobile phase B (chloroform: methanol: water: ammonium hydroxide, 55:39.9:5:0.1, v/v); 95% A for 2 min, linear gradient to 30% A over 18 min and held for 3 min, and linear gradient to 95% A over 2 min and held for 6 min. Sterols and glycerolipids were separated with reverse-phase HPLC using an isocratic mobile phase with an Agilent Zorbax Eclipse XDB-C18 column (4.6 × 100 mm). Quantification of lipid species was accomplished using multiple reaction monitoring (MRM) transitions. Expanded procedures are described in the Supplemental Experimental Procedures.

SUPPLEMENTAL INFORMATION

Supplemental Information includes Supplemental Experimental Procedures, four figures, and three tables and can be found with this article online at http://dx.doi.org/10.1016/j.chom.2015.08.003.

AUTHOR CONTRIBUTIONS

Conceived and designed the experiments: S.G., E.H.E., D.A.F. Performed the experiments: S.G., R.B.C., B.J., B.Z., P.-Y.M., M.C.S.L., N.S., O.C.-F., D.H., T.S.W. Analyzed the data: S.G., E.H.E., K.V.R., D.A.F. Wrote the paper: S.G., D.A.F., with input from other authors. All authors approved the final manuscript.

ACKNOWLEDGMENTS

Funding for this work was provided by the NIH (R01 AI085584 and R01 AI103058 to D.A.F), a postdoctoral award from Novartis for P.-Y.M., and a Burroughs Wellcome carrier development award for M.M.

Received: December 16, 2014
Revised: June 29, 2015
Accepted: August 13, 2015
Published: September 9, 2015

REFERENCES

Adjalley, S.H., Johnston, G.L., Li, T., Eastman, R.T., Ekland, E.H., Eappen, A.G., Richman, A., Sim, B.K., Lee, M.C., Hoffman, S.L., and Fidock, D.A. (2011). Quantitative assessment of *Plasmodium falciparum* sexual development reveals potent transmission-blocking activity by methylene blue. Proc. Natl. Acad. Sci. USA *108*, E1214–E1223.

Ariga, T., McDonald, M.P., and Yu, R.K. (2008). Role of ganglioside metabolism in the pathogenesis of Alzheimer's disease–a review. J. Lipid Res. *49*, 1157–1175.

Asahi, H., Kanazawa, T., Hirayama, N., and Kajihara, Y. (2005). Investigating serum factors promoting erythrocytic growth of *Plasmodium falciparum*. Exp. Parasitol. *109*, 7–15.

Athenstaedt, K., and Daum, G. (2006). The life cycle of neutral lipids: synthesis, storage and degradation. Cell. Mol. Life Sci. *63*, 1355–1369.

Barbosa, A.D., Savage, D.B., and Siniossoglou, S. (2015). Lipid droplet-organelle interactions: emerging roles in lipid metabolism. Curr. Opin. Cell Biol. *35*, 91–97.

Ben Mamoun, C., Prigge, S.T., and Vial, H. (2010). Targeting the lipid metabolic pathways for the treatment of malaria. Drug Dev. Res. *71*, 44–55.

Bobenchik, A.M., Witola, W.H., Augagneur, Y., Nic Lochlainn, L., Garg, A., Pachikara, N., Choi, J.Y., Zhao, Y.O., Usmani-Brown, S., Lee, A., et al. (2013). *Plasmodium falciparum* phosphoethanolamine methyltransferase is essential for malaria transmission. Proc. Natl. Acad. Sci. USA *110*, 18262–18267.

Botté, C.Y., Yamaryo-Botté, Y., Rupasinghe, T.W., Mullin, K.A., MacRae, J.I., Spurck, T.P., Kalanon, M., Shears, M.J., Coppel, R.L., Crellin, P.K., et al. (2013). Atypical lipid composition in the purified relict plastid (apicoplast) of malaria parasites. Proc. Natl. Acad. Sci. USA *110*, 7506–7511.

Boyle, M.J., Wilson, D.W., Richards, J.S., Riglar, D.T., Tetteh, K.K., Conway, D.J., Ralph, S.A., Baum, J., and Beeson, J.G. (2010). Isolation of viable *Plasmodium falciparum* merozoites to define erythrocyte invasion events and advance vaccine and drug development. Proc. Natl. Acad. Sci. USA *107*, 14378–14383.

Bozdech, Z., Llinás, M., Pulliam, B.L., Wong, E.D., Zhu, J., and DeRisi, J.L. (2003). The transcriptome of the intraerythrocytic developmental cycle of *Plasmodium falciparum*. PLoS Biol. *1*, E5.

Cabodevilla, A.G., Sánchez-Caballero, L., Nintou, E., Boiadjieva, V.G., Picatoste, F., Gubern, A., and Claro, E. (2013). Cell survival during complete nutrient deprivation depends on lipid droplet-fueled β-oxidation of fatty acids. J. Biol. Chem. *288*, 27777–27788.

Couper, K.N., Barnes, T., Hafalla, J.C., Combes, V., Ryffel, B., Secher, T., Grau, G.E., Riley, E.M., and de Souza, J.B. (2010). Parasite-derived plasma microparticles contribute significantly to malaria infection-induced inflammation through potent macrophage stimulation. PLoS Pathog. *6*, e1000744.

Drew, M.E., Banerjee, R., Uffman, E.W., Gilbertson, S., Rosenthal, P.J., and Goldberg, D.E. (2008). *Plasmodium* food vacuole plasmepsins are activated by falcipains. J. Biol. Chem. *283*, 12870–12876.

Elabbadi, N., Ancelin, M.L., and Vial, H.J. (1997). Phospholipid metabolism of serine in *Plasmodium*-infected erythrocytes involves phosphatidylserine and direct serine decarboxylation. Biochem. J. *324*, 435–445.

Fivelman, Q.L., McRobert, L., Sharp, S., Taylor, C.J., Saeed, M., Swales, C.A., Sutherland, C.J., and Baker, D.A. (2007). Improved synchronous production of *Plasmodium falciparum* gametocytes *in vitro*. Mol. Biochem. Parasitol. *154*, 119–123.

Garrett, T.A., and Moncada, R.M. (2014). The *Arabidopsis thaliana* lysophospholipid acyltransferase At1g78690p acylates a variety of lysophospholipids including bis(monoacylglycero)phosphate. Biochem. Biophys. Res. Commun. *452*, 1022–1027.

Gault, C.R., Obeid, L.M., and Hannun, Y.A. (2010). An overview of sphingolipid metabolism: from synthesis to breakdown. Adv. Exp. Med. Biol. *688*, 1–23.

Gerold, P., and Schwarz, R.T. (2001). Biosynthesis of glycosphingolipids *de-novo* by the human malaria parasite *Plasmodium falciparum*. Mol. Biochem. Parasitol. *112*, 29–37.

Goñi, F.M., and Alonso, A. (1999). Structure and functional properties of diacylglycerols in membranes. Prog. Lipid Res. *38*, 1–48.

González-Bulnes, P., Bobenchik, A.M., Augagneur, Y., Cerdan, R., Vial, H.J., Llebaria, A., and Ben Mamoun, C. (2011). PG12, a phospholipid analog with potent antimalarial activity, inhibits *Plasmodium falciparum* CTP:phosphocholine cytidylyltransferase activity. J. Biol. Chem. *286*, 28940–28947.

Grzelczyk, A., and Gendaszewska-Darmach, E. (2013). Novel bioactive glycerol-based lysophospholipids: new data – new insight into their function. Biochimie *95*, 667–679.

Guan, Z., Li, S., Smith, D.C., Shaw, W.A., and Raetz, C.R. (2007). Identification of N-acylphosphatidylserine molecules in eukaryotic cells. Biochemistry *46*, 14500–14513.

Haldar, K., Uyetake, L., Ghori, N., Elmendorf, H.G., and Li, W.L. (1991). The accumulation and metabolism of a fluorescent ceramide derivative in *Plasmodium falciparum*-infected erythrocytes. Mol. Biochem. Parasitol. *49*, 143–156.

Hanada, K., Mitamura, T., Fukasawa, M., Magistrado, P.A., Horii, T., and Nishijima, M. (2000). Neutral sphingomyelinase activity dependent on Mg2+ and anionic phospholipids in the intraerythrocytic malaria parasite *Plasmodium falciparum*. Biochem. J. *346*, 671–677.

Hannun, Y.A., and Obeid, L.M. (2011). Many ceramides. J. Biol. Chem. *286*, 27855–27862.

Hara, A., and Radin, N.S. (1978). Lipid extraction of tissues with a low-toxicity solvent. Anal. Biochem. *90*, 420–426.

Igarashi, Y., Kitamura, K., Toyokuni, T., Dean, B., Fenderson, B., Ogawass, T., and Hakomori, S. (1990). A specific enhancing effect of N,N-dimethylsphingosine on epidermal growth factor receptor autophosphorylation. Demonstration of its endogenous occurrence (and the virtual absence of unsubstituted sphingosine) in human epidermoid carcinoma A431 cells. J. Biol. Chem. *265*, 5385–5389.

Inokuchi, J., Nagafuku, M., Ohno, I., and Suzuki, A. (2015). Distinct selectivity of gangliosides required for $CD4^+$ T and $CD8^+$ T cell activation. Biochim. Biophys. Acta *1851*, 98–106.

Kafsack, B.F., Rovira-Graells, N., Clark, T.G., Bancells, C., Crowley, V.M., Campino, S.G., Williams, A.E., Drought, L.G., Kwiatkowski, D.P., Baker, D.A., et al. (2014). A transcriptional switch underlies commitment to sexual development in malaria parasites. Nature *507*, 248–252.

Labaied, M., Dagan, A., Dellinger, M., Gèze, M., Egée, S., Thomas, S.L., Wang, C., Gatt, S., and Grellier, P. (2004). Anti-*Plasmodium* activity of ceramide analogs. Malar. J. *3*, 49.

Lauer, S.A., Rathod, P.K., Ghori, N., and Haldar, K. (1997). A membrane network for nutrient import in red cells infected with the malaria parasite. Science *276*, 1122–1125.

Maceyka, M., and Spiegel, S. (2014). Sphingolipid metabolites in inflammatory disease. Nature *510*, 58–67.

Macrae, J.I., Lopaticki, S., Maier, A.G., Rupasinghe, T., Nahid, A., Cowman, A.F., and McConville, M.J. (2014). *Plasmodium falciparum* is dependent on de novo myo-inositol biosynthesis for assembly of GPI glycolipids and infectivity. Mol. Microbiol. *91*, 762–776.

Mantel, P.Y., Hoang, A.N., Goldowitz, I., Potashnikova, D., Hamza, B., Vorobjev, I., Ghiran, I., Toner, M., Irimia, D., Ivanov, A.R., et al. (2013). Malaria-infected erythrocyte-derived microvesicles mediate cellular communication within the parasite population and with the host immune system. Cell Host Microbe *13*, 521–534.

McNamara, C.W., Lee, M.C., Lim, C.S., Lim, S.H., Roland, J., Nagle, A., Simon, O., Yeung, B.K., Chatterjee, A.K., McCormack, S.L., et al. (2013). Targeting *Plasmodium* PI(4)K to eliminate malaria. Nature *504*, 248–253.

Mi-Ichi, F., Kano, S., and Mitamura, T. (2007). Oleic acid is indispensable for intraerythrocytic proliferation of *Plasmodium falciparum*. Parasitology *134*, 1671–1677.

Nantakomol, D., Dondorp, A.M., Krudsood, S., Udomsangpetch, R., Pattanapanyasat, K., Combes, V., Grau, G.E., White, N.J., Viriyavejakul, P., Day, N.P., and Chotivanich, K. (2011). Circulating red cell-derived microparticles in human malaria. J. Infect. Dis. *203*, 700–706.

Nilsson, S.K., Childs, L.M., Buckee, C., and Marti, M. (2015). Targeting human transmission biology for malaria elimination. PLoS Pathog. *11*, e1004871.

Palacpac, N.M., Hiramine, Y., Mi-ichi, F., Torii, M., Kita, K., Hiramatsu, R., Horii, T., and Mitamura, T. (2004a). Developmental-stage-specific triacylglycerol biosynthesis, degradation and trafficking as lipid bodies in *Plasmodium falciparum*-infected erythrocytes. J. Cell Sci. *117*, 1469–1480.

Palacpac, N.M., Hiramine, Y., Seto, S., Hiramatsu, R., Horii, T., and Mitamura, T. (2004b). Evidence that *Plasmodium falciparum* diacylglycerol acyltransferase is essential for intraerythrocytic proliferation. Biochem. Biophys. Res. Commun. *321*, 1062–1068.

Pankova-Kholmyansky, I., Dagan, A., Gold, D., Zaslavsky, Z., Skutelsky, E., Gatt, S., and Flescher, E. (2003). Ceramide mediates growth inhibition of the *Plasmodium falciparum* parasite. Cell. Mol. Life Sci. *60*, 577–587.

Pattanapanyasat, K., Sratongno, P., Chimma, P., Chitjamnongchai, S., Polsrila, K., and Chotivanich, K. (2010). Febrile temperature but not proinflammatory cytokines promotes phosphatidylserine expression on *Plasmodium falciparum* malaria-infected red blood cells during parasite maturation. Cytometry A *77*, 515–523.

Pelle, K.G., Oh, K., Buchholz, K., Narasimhan, V., Joice, R., Milner, D.A., Brancucci, N.M., Ma, S., Voss, T.S., Ketman, K., et al. (2015). Transcriptional profiling defines dynamics of parasite tissue sequestration during malaria infection. Genome Med. *7*, 19.

Raposo, G., and Stoorvogel, W. (2013). Extracellular vesicles: exosomes, microvesicles, and friends. J. Cell Biol. *200*, 373–383.

Regev-Rudzki, N., Wilson, D.W., Carvalho, T.G., Sisquella, X., Coleman, B.M., Rug, M., Bursac, D., Angrisano, F., Gee, M., Hill, A.F., et al. (2013). Cell-cell communication between malaria-infected red blood cells via exosome-like vesicles. Cell *153*, 1120–1133.

Rottmann, M., McNamara, C., Yeung, B.K., Lee, M.C., Zou, B., Russell, B., Seitz, P., Plouffe, D.M., Dharia, N.V., Tan, J., et al. (2010). Spiroindolones, a potent compound class for the treatment of malaria. Science *329*, 1175–1180.

Salzer, U., and Prohaska, R. (2001). Stomatin, flotillin-1, and flotillin-2 are major integral proteins of erythrocyte lipid rafts. Blood *97*, 1141–1143.

Schaible, U.E., Schlesinger, P.H., Steinberg, T.H., Mangel, W.F., Kobayashi, T., and Russell, D.G. (1999). Parasitophorous vacuoles of *Leishmania mexicana* acquire macromolecules from the host cell cytosol via two independent routes. J. Cell Sci. *112*, 681–693.

Sidhu, A.B., Sun, Q., Nkrumah, L.J., Dunne, M.W., Sacchettini, J.C., and Fidock, D.A. (2007). *In vitro* efficacy, resistance selection, and structural modeling studies implicate the malarial parasite apicoplast as the target of azithromycin. J. Biol. Chem. *282*, 2494–2504.

Silvestrini, F., Lasonder, E., Olivieri, A., Camarda, G., van Schaijk, B., Sanchez, M., Younis Younis, S., Sauerwein, R., and Alano, P. (2010). Protein export marks the early phase of gametocytogenesis of the human malaria parasite *Plasmodium falciparum*. Mol. Cell. Proteomics *9*, 1437–1448.

Slotte, J.P. (2013). Biological functions of sphingomyelins. Prog. Lipid Res. *52*, 424–437.

Taraschi, T.F., Trelka, D., Schneider, T., and Matthews, I. (1998). *Plasmodium falciparum*: characterization of organelle migration during merozoite morphogenesis in asexual malaria infections. Exp. Parasitol. *88*, 184–193.

Tinkelenberg, A.H., Liu, Y., Alcantara, F., Khan, S., Guo, Z., Bard, M., and Sturley, S.L. (2000). Mutations in yeast ARV1 alter intracellular sterol distribution and are complemented by human ARV1. J. Biol. Chem. *275*, 40667–40670.

Tran, P.N., Brown, S.H., Mitchell, T.W., Matuschewski, K., McMillan, P.J., Kirk, K., Dixon, M.W., and Maier, A.G. (2014). A female gametocyte-specific ABC transporter plays a role in lipid metabolism in the malaria parasite. Nat. Commun. *5*, 4773.

van Schaijk, B.C., Kumar, T.R., Vos, M.W., Richman, A., van Gemert, G.J., Li, T., Eappen, A.G., Williamson, K.C., Morahan, B.J., Fishbaugher, M., et al. (2014). Type II fatty acid biosynthesis is essential for *Plasmodium falciparum* sporozoite development in the midgut of *Anopheles* mosquitoes. Eukaryot. Cell *13*, 550–559.

Yagüe, G., Segovia, M., and Valero-Guillén, P.L. (1997). Acyl phosphatidylglycerol: a major phospholipid of *Corynebacterium amycolatum*. FEMS Microbiol. Lett. *151*, 125–130.

Yuan, J., Cheng, K.C., Johnson, R.L., Huang, R., Pattaradilokrat, S., Liu, A., Guha, R., Fidock, D.A., Inglese, J., Wellems, T.E., et al. (2011). Chemical genomic profiling for antimalarial therapies, response signatures, and molecular targets. Science *333*, 724–729.